Original Research Article

Impact of Active Aerodynamic Components on Aerodynamic Efficiency under Varying Conditions

Remon Wang

Dublin High School, 8151 Village Parkway, Dublin, CA 94568, United States

ABSTRACT

Global carbon emissions are at an all-time high in part due to gas vehicles. While efforts to switch to more fuel efficient and electric vehicles are prevalent, these efforts are slow. Simple measures to reduce aerodynamic drag through active aerodynamics would increase each individual vehicle's efficiency, reducing emissions. Active aerodynamic parts alter features of the vehicle's body and its interaction with the oncoming air. While simulations can model these effects, there is limited empirical data from physical tests essential for understanding airflow around real components by addressing uncontrollable variables simulations couldn't. To address this gap, this research aims to answer the questions, *To what extent can a homemade wind tunnel demonstrate aerodynamic flow?* and *To what extent do active aerodynamic components improve aerodynamic efficiency?* Through an experiment involving a wind tunnel and models of F1 rear wings with openable flaps, this paper investigates the effects of active aerodynamics quantitatively and qualitatively. The variables of the drag force equation were measured and experimentally determined, and the drag force of the open and closed configurations were analyzed. Due to the reduced cross-sectional area, the configuration with an open flap exhibited a 0.51% decrease in drag force compared to the control configuration at slow speeds. From the findings, the decrease in drag reduces the air resistance vehicles combat, decreasing fuel consumption to achieve the same speed. This has implications for climate change through automobile users worldwide, as the findings of this study indicate active aerodynamics' drag reduction directly lowers fuel consumption in vehicles.

Keywords: Active Aerodynamics; Wind Tunnel; Drag Reduction; Energy Efficiency; 3D Printing

INTRODUCTION

Cars and other modes of transportation largely contribute to the growing energy crisis and climate change due to pollution. Recent studies from the Intergovernmental Panel on Climate Change found that transportation accounts for 23% of global CO_2 emissions. Within the transport sector, automobiles directly contribute 70% percent of the global CO_2 Those vehicles, especially commercial gas vehicles as well as semi-trucks, are guaranteed to face air-induced drag forces that lower the efficiency of the vehicle and result in higher fuel consumption (1). Currently, vehicles powered by alternative fuel face various challenges, including the development of a battery safe and effective enough

Corresponding author: Remon Wang, E-mail: remonwang2017@gmail.com.

Accepted December 4, 2025
https://doi.org/10.70251/HYJR2348.36807815

to match their gas-powered counterparts (2). Instead, modifying current features of vehicles, such as their shape and therefore aerodynamics, may prove a valuable alternative and easier for implementation.

Many auto manufacturers already have aerodynamics in mind when designing new vehicles. Aerodynamics dictate that the vehicle's shape and features can be designed in a way to reduce those drag forces to raise vehicle efficiency, in turn reducing pollution (3). For example, the truncation of the rear end and the streamlined design of the vehicle significantly smooths out the flow of air and has been in mind since the early 20th century (4). However, different vehicle shapes may be more efficient at different speeds, seen in the four configurations of the Bugatti Veyron, thus calling for modifications to the body shape that active aerodynamics may offer (5).

One promising field of study for reducing pollution in vehicles is the use of active aerodynamics. Active aerodynamics are implemented through features on a vehicle that are able to manipulate components of a vehicle to alter its interaction with the air, which may lead to a significant advancement in vehicle efficiency, safety, and even performance (6). Active aerodynamics only exist within sports like Formula 1 and extremely high-performance sports cars that use it for performance. However, in the future, active aerodynamics may have even more impact when applied to commercial vehicles for its ability to reduce and increase drag (7) When applied to commercial vehicles, energy saved from the reduced drag may accumulate from all vehicles across the globe, slowing the effect of global warming (7). Alternatively, it can increase drag to make sudden deceleration easier and safer for users like seen in the Mclaren Senna (8).

This study aims to investigate the role of active aerodynamic components and how they improve aerodynamic efficiency through reducing frontal area. By utilizing a wind tunnel and 3D printed components, this study expands knowledge on the effect of active aerodynamics through features that decrease the cross-sectional area of a vehicle. This study was guided by the research questions: RQ#1 *To what extent can a homemade wind tunnel demonstrate aerodynamic flow?* and RQ#2 *To what extent do active aerodynamic components improve aerodynamic efficiency?* This research furthers the understanding of the cause and effects of active aerodynamics on drag by experimentally determining the cause and effect of drag in a wind tunnel experiment.

LITERATURE REVIEW

Automotive engineers have long understood that reducing a vehicle's frontal area and improving its streamlined shape decreases drag and increases fuel efficiency. For example, efforts to streamline the shape of public buses have been implemented to reduce their drag, and thus their fuel consumption (9). Kim discovered that by using an optimized and streamlined shape, the drag decreased by 27.4%, which translates to 17.3 kW at 120 km/hr., saving 14610 liters of fuel and about 41.2 tons of CO_2 per year (9). Yet aerodynamics extends far beyond fuel-efficient body shapes, for example, airflow can also be harnessed to generate downforce or reduce drag through specialized wings and surfaces (10). One example is gap fairing, the addition of wings or foils that allows air to pass through a truck's head to its cargo smoothly, which reduces the drag of tractor-trailers by about 7% at highway speeds (11). A similar result has been achieved by Wang (2025), who concluded that a reduction in drag through gap fairing by about 10% would translate to a 5-8% reduction in fuel consumption in standard highway conditions (12).

Over time, deliberate aerodynamic design has evolved from simple streamlining to sophisticated, performance-enhancing features across both racing and consumer vehicles. A major advancement in sophisticated modern vehicle aerodynamics is the rise of active aerodynamics, where components adjust in real time to manipulate airflow. Formula 1's Drag Reduction System (DRS), introduced in 2011, exemplifies this concept: it opens a flap in the rear wing to reduce drag and increase straight-line speed (13, 14). Other active systems can raise flaps to increase drag for improved braking or lower the body to reduce underbody pressure (5). This paper focuses exclusively on active aerodynamic features designed to reduce drag in order to improve fuel efficiency.

Methods for Measuring Drag Force

Common methods to quantify aerodynamics and drag force experimentally include digital models like Computational Fluid Dynamics (CFD) simulations and physical experiments like wind tunnels. CFD simulations measure drag force by replacing the continuous surface one would face in the real world with a discrete "surface" using a grid; with a discrete system established, flow variables are determined and solved only at the grid points: a task that suits computers better than humans (15). Simulations have limitations in measuring aerodynamics because of potential errors

and uncertainties relating to numeric challenges and modeling. Additionally, preparing the geometries and grid mesh for new components takes a significant amount of time, skill, and manual work for users trying to analyze the aerodynamics of a component (16).

Wind tunnels are commonly used in research due to their ability to accurately predict and visualize aerodynamic phenomena (17). Within a wind tunnel, the air flows in one direction under a set speed, and smoke is introduced to visualize the airflow around the object (18). There exist a variety of wind tunnel types. The open loop setup utilizes the surrounding air by drawing in air from one end and releasing it from the other; The closed loop setup recycles the used air in an air-tight loop. The open setup is preferred for its cost efficiency and simplicity, but the closed setup favors accurate high-speed testing (18). They can also vary by how the wind enters the system. A "blower" setup has fans that directly blow air into the testing chamber while a "suck down" setup has fans at the end of the testing chamber that creates airflow by drawing air into it through the testing chamber (18). Wind tunnels can measure drag force through a variety of methods, but most notably and commonly is the use of force sensors that directly measure the amount of drag force the object experiences (19). Arabacı and Kiraz's own force sensor holder (FSH) measures drag by having the sensor hold the component, resulting in a frictionless and lossless measurement of the drag force (19).

METHODS AND MATERIALS

Materials

To conduct this research, proper data from a functioning wind tunnel was required. Proper access to advanced equipment, sensors, or a sophisticated wind tunnel were not available, which prompted the design and creation of a semi-professional wind tunnel. As described by Ansari *et al*. (2014), the constructed wind tunnel resembles an open circuit, suck-down configuration, meaning that air travels in and out of the chamber freely at a controlled speed by the fan sucking air out of the chamber at the end of the setup. This is illustrated in the wind tunnel developed for this study (Figure 1). Inspired by the aforementioned article, the wind tunnel was also made from recycled and household materials (20). A humidifier was connected to a bendable straw, which funnels the mist in a horizontal direction with a flow rate of about 0.785 in^3/s. The test chamber was made using a 5.3in x 5.3in x 8in clear rectangular box by cutting out an additional opening in the bottom and placing it on its side. The main humidifier straw is placed within the testing chamber and is surrounded by parallel straws to fill the opening in order to produce laminar flow for the mist. The Venturi effect, the accelerating of air within the chamber due to change in pressure, was not intentionally implemented due to a lack of tools; changes in pressure cannot be measured and the long straw that connected to the humidifier already ensured laminar flow within the testing chamber. To visualize the airflow, black paper was taped to the back, a light on top of the chamber was placed, and was finished off with a 3.5W fan at the end to draw the mist in the desired direction.

The tested parts were created using a 3D printer with models from Thipilopo (2022) on Printables, an open resource online. The model was of a 2022 Formula 1 rear wing that contains a movable flap in order to mimic the drag reduction system. The .stl file was downloaded and imported to Bambu Studio (21) and was printed with PLA material for its durability and cost efficiency (Figure 2). It should be noted that the model was scaled down to 35% of the original size of the downloaded model in order for it to fit within the wind tunnel.

Data Collection

Two iterations of the wing were tested: one with the flap completely closed, and one with the flap opened approximately 15° to mimic the opening and closing of the active aerodynamic part (Figures 3A and 3B). The

Figure 1. Wind Tunnel Design. Completed wind tunnel with laminar stream, with mist produced by a humidifier with a flow rate of 0.785 in^3/s seen in the 5.3in x 5.3in x 8in clear rectangular box as a 3.5W fan draws the mist out of the tunnel.

testing objects were placed within the testing chamber and the airflow was adjusted to hit the stream of mist. The experiment was repeated three times to minimize errors, and the consistent pattern was observed and recorded. As the experiment was conducted, a camera was positioned in front of the testing chamber to record the airflow patterns for the analysis.

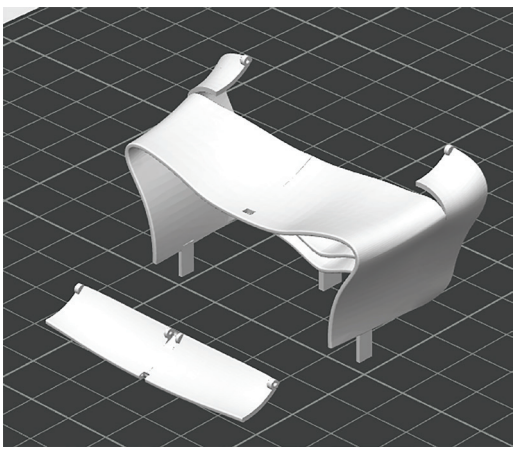

Figure 2. Digital Printed Model of Rear Wing Prototype. 3D model of downsized 2022 Formula 1 rear wing frame and adjustable rear wing flap available through Bambu Labs. Model printed by Bambu Lab P1S using PLA filament.

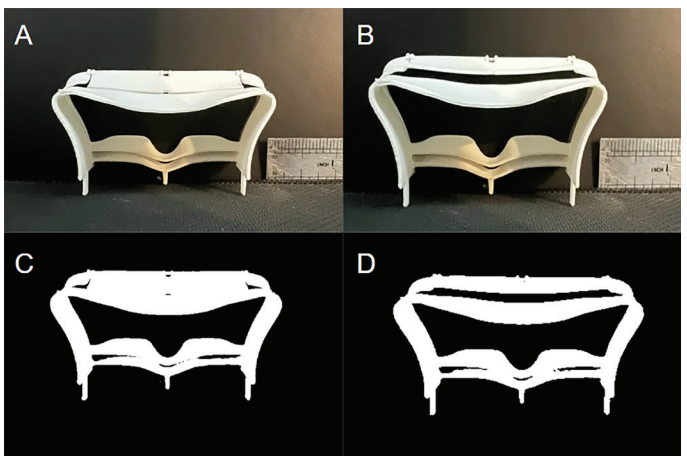

Figure 3. Front-view images of a 3D-printed rear wing of a 2022 F1 car with open and closed flap configurations. (A) Closed-flap configuration, raw photo taken with an iPhone, including a ruler for scale. (B) Open-flap configuration, raw photo taken with an iPhone, including a ruler for scale. (C) Binarized version of panel (A), generated using ImageJ. (D) Binarized version of panel (B), generated using ImageJ.

Qualitative Analysis

During the experiment, photographs of the components' airflow patterns were taken and analyzed. The airflow patterns were visually inspected for instances of laminar and turbulent flow. The humidifier released mist in laminar flow, the smooth, uninterrupted flow of a fluid, through the straw. As the tested component cuts through the laminar mist, it can either guide the mist smoothly, retaining its laminar flow, or leave behind a swirling, chaotic area of turbulent flow. Laminar flow around the object is preferred as it retains the high pressure, fast flowing nature of the air. As the part moves, the air smoothly return to where it once was without creating a low-pressure wake behind the part (22). In contrast, turbulent flow occurs in the low pressure, slow flowing air behind the component. As a large low-pressure area forms behind the part, the pressure exerted does not match that of the high-pressure air accumulated at the front of the part/vehicle, which when combined together yields a net backwards force that contributes a large part to the total drag force as pressure drag (23). The pressure drag, a form of parasitic drag, is accounted for in the coefficient of drag. Laminar and turbulent flow patterns are easily observed within the wind tunnel. Laminar flow, and areas with high pressure, remain fast and smooth while turbulent flow appears chaotic and dispersed, signaling a large low-pressure area.

Quantitative Analysis

The second set of experiments investigated the change in drag force during active aerodynamics. Two sets of experiments were performed to test the difference in drag force based on the aerodynamics. With the open flap, the drag force experienced by the wing reduces accordingly as the air would flow through the gap instead of hitting the wing straight on. To examine the drag force of both configurations, the drag equation, as seen in equation [1], was utilized for both configurations. The equation calls for several variables: the drag force, F (N); the coefficient of drag, C_D (unitless); the air density, ρ (kg/m^3); the air velocity, v (m/s); and the cross sectional surface area, A (m^2).

$$F_D = 0.5 C_D \rho v^2 A \quad [1]$$

The air density is approximately 1.2 kg/m^3 at room temperature and standard pressure (24). The density of the mist that visualizes the airflow within the wind tunnel must also be found and accounted for. The mixture density equation yields the density of a mixture,

$\rho_{mixture}$ (kg/m^3), by summing the volume fraction of the component a_i (unitless) multiplied by their respective densities, ρ_i (kg/m^3). It is known that water has a density of 1000 kg/m^3 and the air an approximate 1.2 kg/m^3, so applying them to equation [2] with the proportion of air and water as 0.99 and 0.1 respectively yields a density of 11.2 kg/m^3

$$\rho_{mixture} = \sum a_i \rho_i \quad [2]$$

The air velocity required additional testing to be determined. A piece of graph paper, where four grids equal to exactly 1 inch, was taped to the black background. The humidifier straw was pinched and once released, the velocity of the mist can be captured and approximated through a slow motion camera, a timer, and its position on the graph paper. Three different time trials were recorded (Table 1). The average wind speed was determined to be around 0.914 kmph or 0.254 meters per second.

Table 1. Trials of wind speed within wind tunnel. Three trials conducted where mist from the humidifier

Trial #	Time (s)	Distance (in)	Speed (in/s)	Speed (m/s)
Trial 1	0.09	1	11.1	0.282
Trial 2	0.11	1	9.09	0.231
Trial 3	0.10	1	10.0	0.254

The cross-sectional surface area was determined through ImageJ, an image processing program. The open and closed configurations of the rear wings were lined up directly in front of a camera in the same orientation in front of a black background and a ruler. Images of both configurations, including a scale bar, were uploaded to ImageJ (Figures 3A and 3B). The images were processed into 8-bit binary images to better contrast the background from the component's frontal area. The inch mark of the ruler was used to set a scale bar for scale. All the remaining white spots, including the ruler, were deleted from the picture, leaving only the cross-sectional surface area of the component visible as white on the binary image (Figures 3C and 3D). ImageJ's "measure" key produced a table which concluded that according to the scale bar set, the component with the flap closed had an area of 2.832 in^2 or 0.001827 m^2 or 1827 mm^2 while the component with the flap opened had an area of 2.611 in^2 or 0.001685 m^2 or 1685 mm^2. The values provided by these tables demonstrate that the 15° opening of the flap decreases the area by approximately 7.804%, which directly affects the experienced drag force.

Lastly, the coefficient of drag was determined through the SimScale, a CFD simulation software commonly used for virtual testing and aerodynamic optimization of designs (25). Using an openly sourced project by ljowen32 (2025) that contains a similar model to the physical model (Figure 4), the simulation determined the coefficient of drag to be around 1.5 and 1.4 for both the closed and open configurations, respectively. Similar modeled wings generally had coefficients of 0.6 and 1.0 for the opened and closed configurations, respectively (26). While the model was similar, the calculated is a reasonable approximation, but a higher value than anticipated.

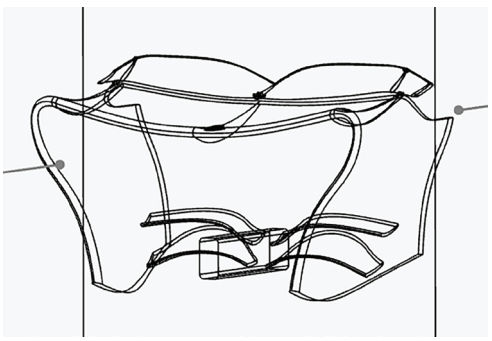

Figure 4. SimScale Model of Rear Wing. Model of 2022 Formula 1 rear wing with closed flaps in SimScale, an aerodynamic computer-aided engineering (CAE) simulation software.

RESULTS

Qualitative Findings

Through visual analysis of the wind trail patterns, a clear distinction is observed between the two configurations. In the closed flap configuration seen in Figure 5A, the mist appeared to hit the wing straight on, which caused the high-pressure air to flow upwards and leave a visible low-pressure area behind the wing that induced turbulent flow, indicated by the chaotic and circular pattern of the mist trail behind the component. In contrast, the open flap configuration seen in Figure 5B clearly flowed through the open flap and generated less of a low-pressure area and therefore less likely to induce turbulent flow. This would indicate that more of the air retained its laminar state as it passed through the wing.

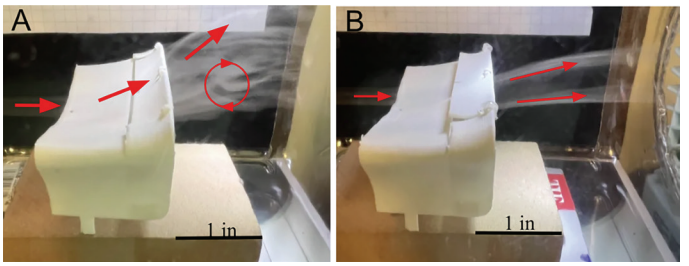

Figure 5. A, Closed Flap Configuration in the Wind Tunnel. Side view of rear wing with closed flaps in the wind tunnel. Visible turbulent flow seen from swirling pattern as mist exits to the right; **B, Open Flap Configuration in the Wind Tunnel.** Side view of rear wing with flaps opened by about 15° above the closed configuration in the wind tunnel. Two streams of visible laminar flow as mist exits to the right.

Quantitative Results

Through drag force experiments, the open flap configuration exhibits a clear decrease in drag force compared to the closed flap configuration. The calculated drag force of the closed flap component experiencing air with little moisture, and thus a lower density, comes to about 9.88×10^{-5} N to the open flap component's 9.83×10^{-5} N (Table 2). On paper, the difference in the forces can attest to the claim that the flaps opening can reduce the drag of the vehicle, as even a semi-professional model yielded an approximate 0.51% decrease in drag force. The calculated drag force of the closed flap component experiencing mist with greater moisture, and thus a higher density, comes to about 9.11×10^{-4} N to the open flap component's 9.18×10^{-4} N (Table II), with a 0.44% decrease.

DISCUSSION

RQ#1: To What Extent can a Homemade Wind Tunnel Demonstrate Aerodynamic Flow?

The qualitative results of this research has shown that the home-made wind tunnel produced visible smoke trails that reflect the expected patterns of visible wind trail left behind by a component interacting with the air (17). The wind tunnel used in this paper largely resembled an open configuration with a "suck down" configuration for its cost efficiency, ease of setup, and clear visuals (18). The mist pattern produced clearly showed the low-pressure wake and the turbulent flow that Leishman (2022) described, with the closed flap configuration leaving a visible low-pressure area indicated by the chaotic pattern of the mist trail and the open flap configuration retaining the laminarity of the mist (22). A low-pressure area behind a component causes increased pressure drag, increasing drag force and therefore increasing fuel consumption. Despite the fact that the wind tunnel of this study produced accurate patterns, it still failed to collect the precise pressure data that an accurate CFD simulation would have provided (15), but as Spalart and Venkatakrishnan (2016) stated, the amount of skill and technology required to run an accurate CFD simulation is immense and was not available (16). However, if access to a device like the Force Sensor Holder that Arabacı and Kiraz (2023) described was available, comparing the drag force between the two configurations would be much simpler and be more accurate (19).

RQ#2: To What Extent do Active Aerodynamic Components Improve Aerodynamic Efficiency?

While this experiment focused on designs similar to an F1 car's drag reduction system (13), the results provide additional evidence that active aerodynamics' subtle changes to the vehicle's shape can affect its performance and be adjusted based on need (27). Seen in this study, the effect from the opening of a rear wing flap, a way to reduce cross sectional area, is demonstrated in that the active aerodynamic component with the open flap resulted in a 0.51% decrease in drag force under normal air conditions and 0.44% decrease in drag under extremely humid conditions when compared to the control configuration with no gap. This small change is in part due to the scaling of the parts and wind speeds to normal part sizes. The printed component is

Table 2. Calculated Drag Force of Active Aerodynamic Components in Different Fluid Conditions

Config.	Density (kg/m^3)	Windspeed^2*C_D (m^2/s^2)	Area (m^2)	Force (N)
Open – Air	1.2	0.097	0.00169	9.83×10^{-5}
Open – Mist	11.0	0.097	0.00169	9.18×10^{-4}
Closed – Air	1.2	0.090	0.00183	9.88×10^{-5}
Closed - Mist	11.2	0.090	0.00183	9.22×10^{-4}

about 2.7 inches wide, about 14.7 times smaller than an F1 car's minimum rear wing size of about 39.6 inches. Additionally, the wind speed, 0.568 mph is 70.43 times slower than normal civilian speed, about 40 mph. When compared to findings in other studies, despite not being the same component, this decrease in drag when a feature is modified for drag-reducing aerodynamics is also seen in the gap fairings on trucks (11). The approximately 0.5% drag reduction found in this research differs from Lazar's (2025) approximate 40% reduction in drag force as their experiment was to real scale and speed only achieved in F1 as well as utilized smaller coefficients of drag of approximately 0.6 and 1 for open and closed configurations, respectively (26). Despite the small change in drag force captured, it allows vehicles to either produce more speed or spend less fuel to achieve the same speed. As more and more vehicles adopt such components, individual fractional gains in fuel efficiency would add up to an unignorable decrease in the global energy consumption (7). Lastly, these results still bring value to physical wind tunnel tests such as the one conducted in this study and additionally can be replicated for educational purposes due to the low cost set up.

Limitations & Future Work

Though it is true that this experiment was conducted in a rudimentary manner that may not reflect actual conditions due to limitations of the study. First, the airspeed is extremely slow compared to actual driving speed, as the wind tunnel and electric fan simply could not produce such high speeds. As the velocity of the air is squared in the equation, this potentially may lead to significant differences in percent drag reduced. Additionally, the variables used in the drag force equation, although carefully yielded through procedures, may still be erroneous. Due to a lack of advanced equipment and materials, the airspeed within the wind tunnel cannot be guaranteed to stay perfectly at a constant 0.254 m/s. This may cause the fluid velocity, v, in the drag equation to be slightly faulty and therefore may produce an error in the total drag force experienced. However, as the error in wind speed was insignificant enough in addition to being used for both the open and closed configurations, the potential error in drag reduction percent due to inaccurate wind speed may be ruled out. Similarly, the C_D generated by the SimScale simulation may also be inaccurate to the printed component as they were not identical models. However again, if such errors were present, they were present in both configurations and thus caused no significant errors to the drag reduction percent. In addition to the drag equation, the lack of equipment also affected the data about pressure changes in the testing chamber. With proper equipment, high- and low-pressure areas may be captured more accurately and a numerical analysis may even be performed. Despite that, the visual inspection still proved useful as areas of high and low pressures were able to be approximated by qualitative analysis. Though even with all the above considered, the drag force equation may not perfectly explain all the benefits an active aerodynamic system may provide to the automotive industry. Advanced fluid mechanics equations such as the Navier-Stokes equation that accounts for a lot more variables may offer a grander picture of the phenomenon exhibited in the testing chamber, but due to insufficient equipment and therefore inaccurate variables, cannot be used for this research. However, the drag force equation's constant of drag still accounted for the parasitic drag forces such as pressure and skin friction drag, which allowed the calculated drag force to be extremely similar to the actual drag force experienced by the component. Despite limitations mentioned above, the study provides insight on the impact of active aerodynamic components on a vehicle's performance. Future work should utilize a wind tunnel with higher speeds to further highlight the contrast between the open and closed configurations. Future work should also utilize CFD simulations more accurately in order to approximate a more realistic coefficient of drag for both configurations.

CONCLUSION

This study attests to the benefits of active aerodynamics within the context of efficiency and sustainability of vehicles. Less drag force allows the vehicle to use less energy when combating air resistance to achieve the same speed, which leads to the usage of smaller amounts of fuel of any kind. The solution, with more refinement on its cost and safety, may be readily applied to vehicles like sedans and coupes that can accommodate and benefit from such active aerodynamic components.

Not every vehicle will have wings akin to that in the study or even a rear end that accommodates a wing at all but said moving flap may be implemented elsewhere to reduce drag. In addition, the findings of this study may be applied in its opposite direction: purposely inducing drag to allow better braking and safety of the vehicle using flap-like protrusions that increase the cross-sectional area and therefore drag. Already implemented

on cars like the Pagani Huayra, these spoilerons and flaps may offer more downforce at high speeds and aid in braking by creating more drag.

ACKNOWLEDGMENTS

Thank you for the guidance of Dr. Adrian Nat Gentry from Purdue University in the development of this research paper.

CONFLICT OF INTEREST

The author declares no conflicts of interest related to this work

REFERENCES

1. Jaramillo P, *et al*. Transport. Mitigation of Climate Change. Contribution of Working Group III to the Sixth Assessment Report of the Intergovernmental Panel on Climate Change. Cambridge: Cambridge Univ Press; 2022; p. 1049-1061.
2. Ornes S. The tricky challenge holding back electric cars. Proceedings of the National Academy of Sciences. 2021; 118 (26): e2109654118. https://doi.org/10.1073/pnas.2109654118
3. Zhang B. A study on aerodynamics of ultra-efficient cars. *J Phys Conf Ser*. 2023; 2634 (1): 012010. https://doi.org/10.1088/1742-6596/2634/1/012010
4. Hucho WH. Aerodynamics of road vehicles: from fluid mechanics to vehicle engineering. Amsterdam: Elsevier; 2013; 1(11).
5. Piechna J. A review of active aerodynamic systems for road vehicles. *Energies*. 2021; 14 (23): 7887. https://doi.org/10.3390/en14237887
6. Corno M, *et al*. Performance assessment of active aerodynamic surfaces for comfort and handling optimization in sport cars. *IEEE Trans Control Syst Technol*. 2015; 24 (1): 189-99. https://doi.org/10.1109/TCST.2015.2424158
7. Connolly MG, *et al*. Drag reduction technology and devices for road vehicles: A comprehensive review. *Heliyon*. 2024; 10 (13). https://doi.org/10.1016/j.heliyon.2024.e33757
8. Kurec K, *et al*. Advanced modeling and simulation of vehicle active aerodynamic safety. *J Adv Transp.* 2019; 2019 (1): 7308590. https://doi.org/10.1155/2019/7308590
9. Kim CH. A streamlined design of a high-speed coach for fuel savings and reduction of carbon dioxide. *International Journal of Automotive Engineering*. 2011; 2 (4): 101-7. https://doi.org/10.20485/jsaeijae.2.4_101
10. RAKESH MD. A SEMINAR REPORT on SHAPE OPTIMIZATION OF A CAR BODY FOR DRAG REDUCTION AND TO INCREASE DOWNFORCE. Available from: https://www.researchgate.net/publication/301674058_SHAPE_OPTIMIZATION_OF_A_CAR_BODY_FOR_DRAG_REDUCTION_AND_TO_INCREASE_DOWNFORCE/citation/download (accessed on 2025-11-11)
11. Cooper KR, Leuschen J. Model and full-scale wind tunnel tests of second-generation aerodynamic fuel saving devices for tractor-trailers. *SAE Tech Paper*. 2005; p. 3512. https://doi.org/10.4271/2005-01-3512
12. Wang R. Study on Aerodynamic Optimisation of Medium-Duty Trucks: Drag Control and Fuel Efficiency Improvement. In2025 2nd International Conference on Electrical Engineering and Intelligent Control. Atlantis Press. (EEIC 2025). 2025; p.876-885. https://doi.org/10.2991/978-94-6463-864-6_76
13. Azmi ARS, *et al*. IOP Conf Ser Mater Sci Eng. 2017; 243: 012030. https://doi.org/10.1088/1757-899X/243/1/012030
14. Zoco JU, *et al*. Design, Simulation, Construction and Testing of a Formula One Rear Wing with Drag Reduction System (DRS). Available from: https://academica-e.unavarra.es/entities/publication/0507cf9c-8052-4a59-91a9-fb1497f0a0f7 (accessed on 2025-11-11)
15. Bhaskaran R, *et al*. Introduction to CFD basics. Ithaca (NY): Cornell Univ, Sibley School of Mechanical and Aerospace Engineering. 2002; p. 1-21.
16. Spalart PR, *et al*. On the role and challenges of CFD in the aerospace industry. *Aeronaut J*. 2016; 120 (1223): 209-32. https://doi.org/10.1017/aer.2015.10
17. Sathish S. Wind tunnel testing and modeling implications of an advanced turbine cascade. arXiv preprint arXiv. 2024. p. 2407.
18. Ansari A, *et al*. Drag force analysis of car by using low speed wind tunnel. *Int J Eng Res Rev*. 2014; p. 144-9.
19. Arabacı S, *et al*. A new force measurement mechanism in wind tunnel: CFD and experimental validation on a cylinder. *J Sci Rep-A*. 2023; (053): p. 16-27. https://doi.org/10.59313/jsr-a.1248990
20. Huckans JH, *et al*. A Wind Tunnel in Your Classroom: The Design and Implementation of a Portable Wind Tunnel for Use in the Science Classroom. arXiv preprint physics. 2002; p.0208039.
21. Bambu Lab. Bambu Studio [computer program]. Version 1.9.4. Shenzhen (China): Bambu Lab; 2025. Available from: https://bambulab.com (accessed on 2025-11-11)
22. Leishman JG. Bluff body flows. In: Introduction to

Aerospace Flight Vehicles. Daytona Beach (FL): Embry-Riddle Aeronautical Univ; 2022. ISBN: 979-8-9852614-0-0.

23. Choi H, *et al*. Aerodynamics of heavy vehicles. *Annu Rev Fluid Mech*. 2014; 46 (1): 441-68. https://doi.org/10.1146/annurev-fluid-011212-140616
24. Wang Xiao-lei, *et al*. "Research on Air density Measurement for measuring weights." 20th IMEKO World Congress. 2012. Available from: https://www.imeko.org/publications/tc3-2010/IMEKO-TC3-2010-033.pdf (accessed on 2025-11-11)
25. SimScale GmbH. SimScale [computer program]. Version 3.5. Munich: SimScale GmbH; 2025. Available from: https://www.simscale.com (accessed on 2025-11-11)
26. LAZAR, IKRAM. "Aerodinamica del Drag Reduction System in Formula 1." Available from: https://thesis.unipd.it/handle/20.500.12608/1/browse type=relationCourse&sort_by=ASC&order=1&rpp=20&etal=-1&authority=co516&starts_with=O&offset=6 (accessed on 2025-11-11)
27. Seljak G. Race car aerodynamics. 2008. Available from: https://porschecarshistory.com/wp-content/old/Books/Gregor%20Seljak/Race_Car_Aerodynamics.pdf (accessed on 2025-11-11).